Ultrastructural Colocalization of Tyrosinated and Detyrosinated α-Tubulin in Interphase and Mitotic Cells

Gustaaf Geuens,* Gregg G. Gundersen,‡ Rony Nuydens,* Frans Cornelissen,* Jeannette Chloe Bulinski,‡ and Marc DeBrabander*

*Department of Life Sciences, Janssen Pharmaceutica Research Laboratories, Beerse, Belgium; and
‡Department of Biology and Molecular Biology Institute, University of California, Los Angeles, California 90024

Abstract. Immunofluorescence with specific peptide antibodies has previously established that tyrosinated (Tyr) and detyrosinated (Glu) tubulin, the two species generated by posttranslational modification of the COOH-terminus of α-tubulin, are present in distinct, but overlapping, subsets of microtubules in cultured cells (Gundersen, G. G., M. H. Kalnoski, and J. C. Bulinski, 1984, *Cell*, 38:779–789). Similar results were observed by light microscopic immunogold staining in the two cell types used in this study, CV_1 and PtK_2 cells: most microtubules were stained with the Tyr antibody, whereas only a few were stained with the Glu antibody. We have examined immunogold-stained preparations by electron microscopy to extend these results. In general, electron microscopic localization confirmed results obtained at the light microscopic level: the majority of the microtubules in CV_1 and PtK_2 cells were nearly continuously labeled with the Tyr antibody, whereas only a few were heavily labeled with the Glu antibody. However, in contrast to the light microscopic staining, we found that all microtubules of interphase and mitotic CV_1 and PtK_2 cells contained detectable Tyr and Glu immunoreactivity at the electron microscopic level. No specific localization of either species was observed in microtubules near particular organelles (e.g., mitochondria or intermediate filaments). Quantification of the relative levels of Glu and Tyr immunoreactivity in individual interphase and metaphase microtubules showed that all classes of spindle microtubules (i.e., kinetochore, polar, and astral) contained nearly the same level of Glu immunoreactivity; this level of Glu immunoreactivity was lower than that found in all interphase microtubules. Most interphase microtubules had low levels of Glu immunoreactivity, whereas a few had relatively high levels; the latter corresponded to morphologically sinuous microtubules. Quantification of the relative levels of Tyr and Glu immunoreactivity in segments along individual microtubules suggested that the level of Tyr (or Glu) tubulin in a given microtubule was uniform along its length. Understanding how microtubules with different levels of Tyr and Glu tubulin arise will be important for understanding the role of tyrosination/detyrosination in microtubule function. Additionally, the coexistence of microtubules with different levels of the two species may have important implications for microtubule dynamics in vivo.

TUBULIN, the substituent protein of microtubules, undergoes a unique posttranslational modification, called tyrosination (2, 3). This modification consists of the removal and subsequent readdition of the COOH-terminal tyrosine residue to the α-subunit of tubulin, such that tubulin exists in two biochemically distinct forms in tissues and cultured cells from a variety of organisms. The detyrosinated (Glu)[1] and tyrosinated (Tyr) tubulins contain, respectively, a glutamic acid or a tyrosine as their COOH-terminal residue. Previously, the in vitro behavior of these tubulins has been investigated (1, 12, 15), and changes in their levels have been correlated with several differentiative processes in cultured cells and in tissues (2, 4, 13, 14, 16, 17). Nonetheless, the function of this modification remains obscure.

We previously prepared two peptide antibodies (Glu and Tyr antibodies) that reacted specifically with the Glu or the Tyr form of α-tubulin. By light microscopic immunolocalization of these species in cultured cells, we demonstrated that the Glu and Tyr forms of tubulin exist in distinct, but overlapping, subsets of total cellular microtubules in both interphase and mitotic cells (7, 8).

Although these studies presented tantalizing evidence regarding the in vivo segregation of the Glu and Tyr forms of tubulin, the immunofluorescence technique used left many

1. *Abbreviations used in this paper:* CPA, carboxypeptidase A; GAR-G5, 5-nm colloidal gold-labeled goat anti-rabbit IgG; GARa-G5, 5-nm colloidal gold-labeled goat anti-rat IgG; GAR-G10, 10-nm colloidal gold-labeled goat anti-rabbit IgG; Glu, detyrosinated α-tubulin; Tyr, tyrosinated α-tubulin; TBS, Tris-buffered saline.

questions unanswered. For example, in interphase African green monkey kidney cells, individual microtubules could be resolved which were stained only with the Tyr antibody, only with the Glu antibody, or with both antibodies. Although this suggests that some microtubules are composed of only one of the two species of α-tubulin, it is possible that the other species is present, but at a level below the limit of detection of immunofluorescence. Immunolabeling at the electron microscopic level was previously used for the detection of a species present in minor amounts along microtubules (5) and should be amenable to detection of low amounts of Glu or Tyr tubulin in individual microtubules. Furthermore, the discrete nature of the immunogold label should allow the quantification of the relative levels of each species along a microtubule.

The resolution with which Glu and Tyr tubulin were localized in the previous immunofluorescence studies could be extended by ultrastructural immunolocalization. Electron microscopic immunolocalization would permit the observation of organelles, such as mitochondria, or other cytoskeletal elements, whose distribution might be correlated with the distribution of Glu- or Tyr-containing microtubules. The increased resolution afforded by electron microscopy might be especially useful in the analysis of mitotic cells in which close packing of spindle microtubules made it difficult to address several questions at the light microscopic level (8). For example, is the distribution of Glu and Tyr tubulin uniform throughout the spindle? Are there distinct Glu and Tyr microtubules in spindles, as are found in interphase cells? What is the distribution of Glu and Tyr tubulin on different classes of spindle microtubules, e.g., on kinetochore and nonkinetochore microtubules? Is Glu (or Tyr) tubulin enriched near the poles? Near the kinetochores? Clearly the resolution of electron microscopy as well as the ability to identify kinetochores and centrosomes would aid us in interpreting immunostaining experiments performed with mitotic cells.

In this report, we present the electron microscopic immunolocalization of Glu and Tyr α-tubulin in two types of cultured mammalian cells. Our results have confirmed and extended the interpretations based on our previous light microscopic results, and have allowed a precise and quantitative assessment of the distribution of these two tubulins in vivo.

Materials and Methods

Cells

African green monkey (CV_1) and rat kangaroo (PtK_2) kidney cells were cultured on plastic petri dishes as previously described (5).

Fixation

All fixation steps were performed at room temperature. Cells were fixed and permeabilized by a 1-min treatment with 1% Triton X-100 (Sigma Chemical Co., St. Louis, MO) and 0.5% glutaraldehyde in buffer I (Hanks' buffered salt solution containing 5 mM Pipes, 2 mM $MgCl_2$, and 2 mM EGTA, pH 6). Cells were fixed further with 0.5% glutaraldehyde for 10 min in buffer I, washed in buffer I, and then permeabilized again with 0.5% Triton X-100 for 30 min in buffer I. Unreacted aldehyde groups were reduced in a 15-min treatment with 0.5 mg/ml $NaBH_4$ in buffer I. Fixation and extraction conditions were chosen after varying glutaraldehyde and Triton concentrations to achieve optimal preservation of structure and permeability to antibodies. To facilitate the examination of cells in these experiments, we used Nanovid microscopy (6), a light microscopic technique using bright-field optics at maximum numerical aperture and electronic contrast enhancement of the image recorded by a high-resolution video camera (model C-1966; Hamamatsu Corp., Middlesex, NJ).

For some experiments, preparations of fixed and extracted cells were treated with carboxypeptidase A (CPA) before antibody incubations, as previously described (7). CPA treatment removes only COOH-terminal tyrosine residues from α-tubulin, yielding completely detyrosinated α-tubulin (7, 13, 15).

Immunogold Staining

All steps were carried out at room temperature. Fixed cells were stained with antibodies diluted in Tris-buffered saline (TBS; 10 mM Tris, 140 mM NaCl, pH 7.6) as follows: After a 30-min incubation with a 1/20 dilution of normal goat serum, cells were incubated with a 1/200 dilution of either Glu or Tyr rabbit antisera in 1% normal goat serum overnight. For double-label experiments, fixed cells were incubated simultaneously or consecutively (no differences were observed between these) with a 1/200 dilution of Glu rabbit antisera and a 1/200 dilution of an affinity-purified rat monoclonal antibody, designated YL 1/2, which has been shown to be specific for Tyr tubulin (11, 21). YL 1/2 was the generous gift of Dr. J. V. Kilmartin (MRC, Cambridge). Several dilutions of each antibody were tested in the immunostaining protocol; the dilutions used were those at which maximum specific labeling was obtained. After washing with TBS, cells were incubated for 3 h with 20 mM Tris, 140 mM NaCl, 0.1% BSA, pH 8.2, containing a 1/2 dilution of 5-nm colloidal gold-labeled goat anti-rabbit IgG (GAR-G5; Janssen Life Sciences Products, Beerse, Belgium). For double-labeled preparations, second antibodies were 5-nm colloidal gold-labeled goat anti-rat IgG (GARa-G5) and 10-nm colloidal gold-labeled goat anti-rabbit IgG (GAR-G10). No difference in staining was observed if GAR-G5 and GARa-G10 were used to detect the rabbit and rat antibodies, respectively.

Stained preparations were examined at both the light and electron microscopic levels. For light microscopy we used Nanovid microscopy as detailed in DeBrabander et al. (6). This provided us with a qualitative assessment of the staining and also allowed us to choose specific cells to investigate at higher resolution in the electron microscope. For electron microscopy, stained and washed preparations were postfixed with 1% glutaraldehyde in buffer I for 10 min, treated with 2% OsO_4 for 30 min, impregnated with 0.5% uranyl acetate for 30 min, dehydrated with ethanol (70–100%), and embedded in Epon (Shell Chemical Co.). Ultrathin sections were examined and photographed with a Philips EM410.

Quantification

To quantify the amount of Glu or Tyr immunoreactivity on single microtubules in double-labeled preparations, representative microtubules were photographed at high contrast and the resulting micrographs were then scanned with a Quantimet 900 image analyzer (Cambridge Instruments, Cambridge, England). This was accomplished by first outlining the microtubule to be analyzed with the light pen and then measuring its length. The gold particles lying within this region were detected using an appropriate grey level threshold. The area and the roundness of these particles were measured. To analyze clustered particles, objects with an area and roundness factor greater than prespecified limits were extracted. Using successive erosion and inverse skeletonization operations, the clusters were separated into individual particles. Counts were reported both as an average value and a range of observed values.

Results

Light Microscopic Localization

The protocol we used for electron microscopic localization of Tyr and Glu tubulin differed in two ways from the protocol we had previously used for immunofluorescence localization (7–9): (*a*) glutaraldehyde fixation vs. methanol fixation and (*b*) immunogold detection vs. immunofluorescence detection. In addition, two cell lines were used that we had not examined previously. Accordingly, we first examined the distribution of Tyr and Glu tubulin in immunogold-stained cells (fixed and stained as for electron microscopic localization) using electronic enhancement of bright field images recorded on a high resolution video camera. This combination of techniques has been referred to as Nanovid microscopy (6).

The patterns obtained by Nanovid microscopy of both CV_1 and PtK_2 cells, immunogold stained with the Tyr and Glu antibodies (Fig. 1), resembled immunofluorescence patterns of the same cells (data not shown) and were similar to distributions reported previously for other cultured cell lines (7–9). In both the CV_1 and PtK_2 cells, the Tyr antibody intensely labeled most interphase microtubules and all classes of spindle microtubules (Fig. 1, *a–c*). In fact, the Tyr antibody appeared to label the entire microtubule array; although, it is possible that a small number of microtubules were not labeled and hence escaped detection. We previously found by double immunofluorescence that some interphase microtubules were not labeled with the Tyr antibody (7). In contrast to the Tyr antibody, the Glu antibody labeled far fewer interphase microtubules in both cell types and many of these microtubules were sinuous (Fig. 1, *d* and *f*). In some cases patchy labeling of single microtubules was observed with the Glu antibody (*arrow*, Fig. 1 *f*); this patchy labeling was not detected in previous immunofluorescence studies (7, 9).

Nanovid microscopy of mitotic cells stained with the Tyr and Glu antibodies yielded results similar to previous immunofluorescence results (7, 8). In metaphase spindles, all classes of microtubules were labeled heavily with the Tyr antibody (Fig. 1 *b*). Although the Glu antibody labeled half-spindle fibers, it appeared to label astral fibers faintly or not at all (Fig. 1 *e*). These results show that the different fixation and staining protocols used in the present study yielded very similar labeling patterns to those obtained previously (7–9). The one significant qualitative difference, namely the patchy labeling of some microtubules with the Glu antibody, may result from the discrete signal afforded by immunogold staining, since it was not detected in the same cells stained by immunofluorescence (data not shown).

The microtubules of CV_1 cells consistently showed more Glu staining than those of PtK_2 cells (compare Fig. 1 *d* with Fig. 1 *f*). This was also true for mitotic spindle staining of CV_1 vs. PtK_2 cells (data not shown). In the >20 different cell lines we have examined, we have found by immunofluorescence that the number of microtubules labeled with the

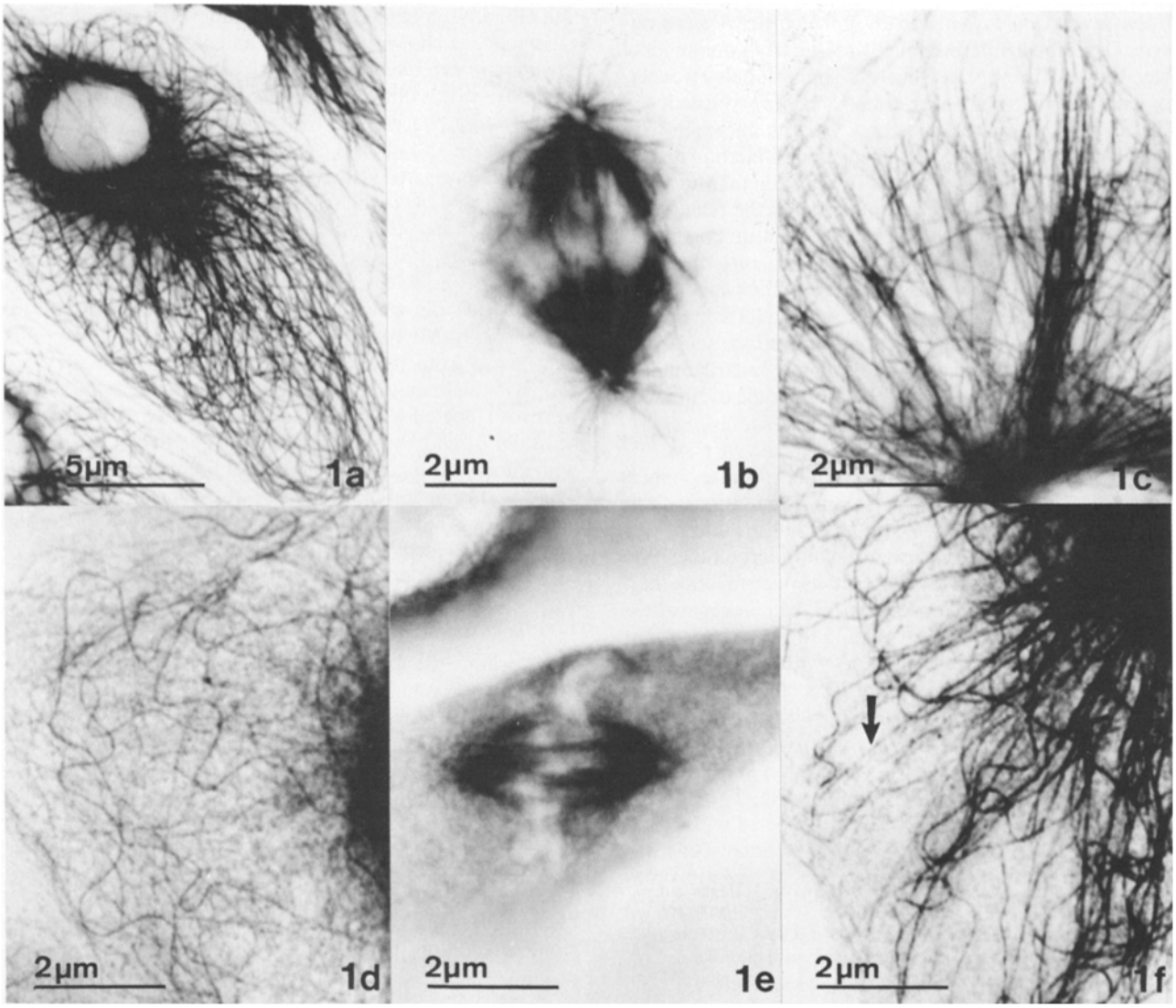

Figure 1. Nanovid ultramicroscopy of PtK_2 and CV_1 cells. Cells were stained with Tyr (*a–c*) or Glu (*d–f*) rabbit antibodies followed by colloidal gold second antibody (GAR-G10). Images were obtained with a video camera as described in Materials and Methods. (*a* and *d*) PtK_2 interphase cells. (*b* and *e*) PtK_2 mitotic cells. (*c* and *f*) CV_1 interphase cells. Arrow in *f* indicates patchy immunogold labeling.

Glu antibody is always less than that labeled with the Tyr antibody; also, the number of microtubules labeled with the Glu antibody varies among cell lines, such that some cell lines have essentially no distinctly labeled microtubules, while others have many (unpublished results). The two cell lines used in this study fall in the lower (PtK_2) to upper (CV_1) range with regard to the amount of Glu staining each possesses; thus, results obtained from these cell lines would be expected to be representative of a wide range of cell types.

Electron Microscopic Localization: Single Label

Fig. 2 shows electron micrographs of thin sections through CV_1 and PtK_2 cells stained with either the Glu or the Tyr antiserum followed by GAR-G5. The conditions of fixation and antibody staining were identical to those used in preparing the cells for light microscopy (Fig. 1). In both CV_1 and PtK_2 cells, almost all interphase microtubules were heavily labeled with the Tyr antibody (Fig. 2, *a*, *c*, and *e*) and only sparsely labeled with the Glu antibody (Fig. 2, *b*, *d*, and *f*). In fact, the extent of labeling of most microtubules with the Glu antibody was so low and of such a discontinuous nature that few microtubules outlined by gold particles were observed. Occasional microtubules were nearly continuously labeled by the Glu antibody; that these microtubules were labeled to a greater extent than most of the microtubules is clearly evident in micrographs of CV_1 cells in which they appear as distinct and traceable microtubules (arrows in Fig. 2 *b*). Thus, immunolocalization of Tyr and Glu tubulin at the electron microscopic level confirms most of the results obtained at the light microscopic level. However, in contrast to previous light microscopic data, in which some microtubules appeared not to be stained with one of the two antibodies (Fig. 1; also see references 7 and 9), the electron microscopic examination of single-labeled preparations suggested that all microtubules possess some staining (even though it may be at a very low level) with both antibodies. This will become even more apparent from the double-staining experiments described in the next section.

Several additional features of the results from the single-label experiments are worthy of mention. First, almost all of the gold particles in cells labeled with either the Glu or Tyr antibodies were found in association with microtubules. We observed no labeling of microfilaments or intermediate filaments; similarly, we found no labeling of cellular organelles, e.g., mitochondria (see Fig. 5). Second, the relative amount of labeling of individual microtubules with either antibody appeared to be independent of the location of the microtubule in the cell. Thus, microtubules near the periphery of the cell had roughly similar amounts of Tyr reactivity as those near the centrosome (compare Fig. 2, *a* and *c*); a similar result was found for the Glu antibody (compare Fig. 2, *b* and *d*). Finally, note that the centrioles were not labeled with either antibody (Fig. 2, *c–f*; also, see Fig. 4). Presumably this was due to limited penetration of the antibodies into centrosomes in glutaraldehyde-fixed cells; we have observed that centrosomes (and presumably centrioles) are labeled in immunofluorescent stained preparations of methanol-fixed cells (8, 9) but not in analogously stained, glutaraldehyde-fixed cells (unpublished results).

The specificities of the antibodies used in this study have previously been described in detail (7, 8) and were confirmed for the immunogold labeling procedure used in the present study. As mentioned above, the only cellular structures labeled with immunogold were microtubules. Only a few gold particles were found free in the cytoplasm (Fig. 2). These presumably represent either staining of unextracted, fixed monomeric tubulin or staining of microtubules just outside the plane of the section. Control experiments in which cells were stained with preimmune sera yielded very low levels of staining, and the few gold particles associated with the cells were randomly distributed on cellular structures (Fig. 3, *a* and *b*). As another control experiment, we treated fixed, extracted cells with CPA to remove the COOH-terminal tyrosine residues from the cellular tubulin before staining with the antibodies. As shown in Fig. 3 *c*, pretreatment with CPA increased the labeling with the Glu antibody such that all microtubules were continuously labeled. Pretreatment with CPA reduced labeling with the Tyr antibody to the same low level as was observed for staining with preimmune serum (data not shown). These controls confirmed that the immunogold staining with the Glu and Tyr antibodies accurately reflected the distribution of Glu and Tyr tubulin.

We have also performed immunogold localization of Tyr and Glu tubulin at the ultrastructural level in metaphase mitotic cells, as shown in Fig. 4. None of the microtubules in the spindle exhibited high levels of reactivity with the Glu antibody, as was observed for a small population of microtubules in interphase cells (e.g., compare Fig. 4 *b* with Fig. 2 *b*). Instead, all classes of spindle microtubules exhibited very high levels of Tyr reactivity and only low levels of Glu reactivity (Fig. 4, *a* and *b*). Kinetochore microtubules were labeled very heavily and nearly continuously with the Tyr antibody (Fig. 4 *a*, inset) and less extensively with the Glu antibody (Fig. 4 *b*, inset). Nonetheless, all kinetochore microtubules did show detectable immunostaining with the Glu antibody. Microtubules originating at the pole, but radiating away from the half-spindle (astral microtubules), as well as nonkinetochore microtubules in the half-spindle, were also labeled with both the Tyr and Glu antibodies (Fig. 4, *a* and *b*) and showed nearly the same extent of labeling with the two antibodies as did kinetochore microtubules (see Table I). That astral microtubules were labeled with the Glu antibody was somewhat surprising, since they were not detectably labeled using indirect immunofluorescence (8) or Nanovid microscopy (Fig. 1).

Electron Microscopic Localization: Double Label

To determine the distribution of Tyr and Glu tubulin on individual microtubules, we double-stained cells for these two species. In these experiments, we used the rabbit antibody specific for Glu tubulin and the rat monoclonal antibody specific for Tyr tubulin; reactivity of each antibody was then detected with the appropriate second antibodies conjugated to different sizes of colloidal gold. In Fig. 5, the Tyr antibody staining was visualized with 5-nm colloidal gold, while the Glu antibody staining was visualized with 10-nm colloidal gold.

Results from the double-labeling experiments confirmed those performed with the single label: all microtubules in either PtK_2 cells (Fig. 5, *a* and *b*) or CV_1 cells (Fig. 5, *c* and *d*) were labeled with both Glu and Tyr antibodies. In addition, by using both antibodies, individual microtubules appeared to be continuously labeled in both interphase (Fig. 5, *a* and *c*) and mitotic cells (Fig. 5, *b* and *d*), showing that Tyr

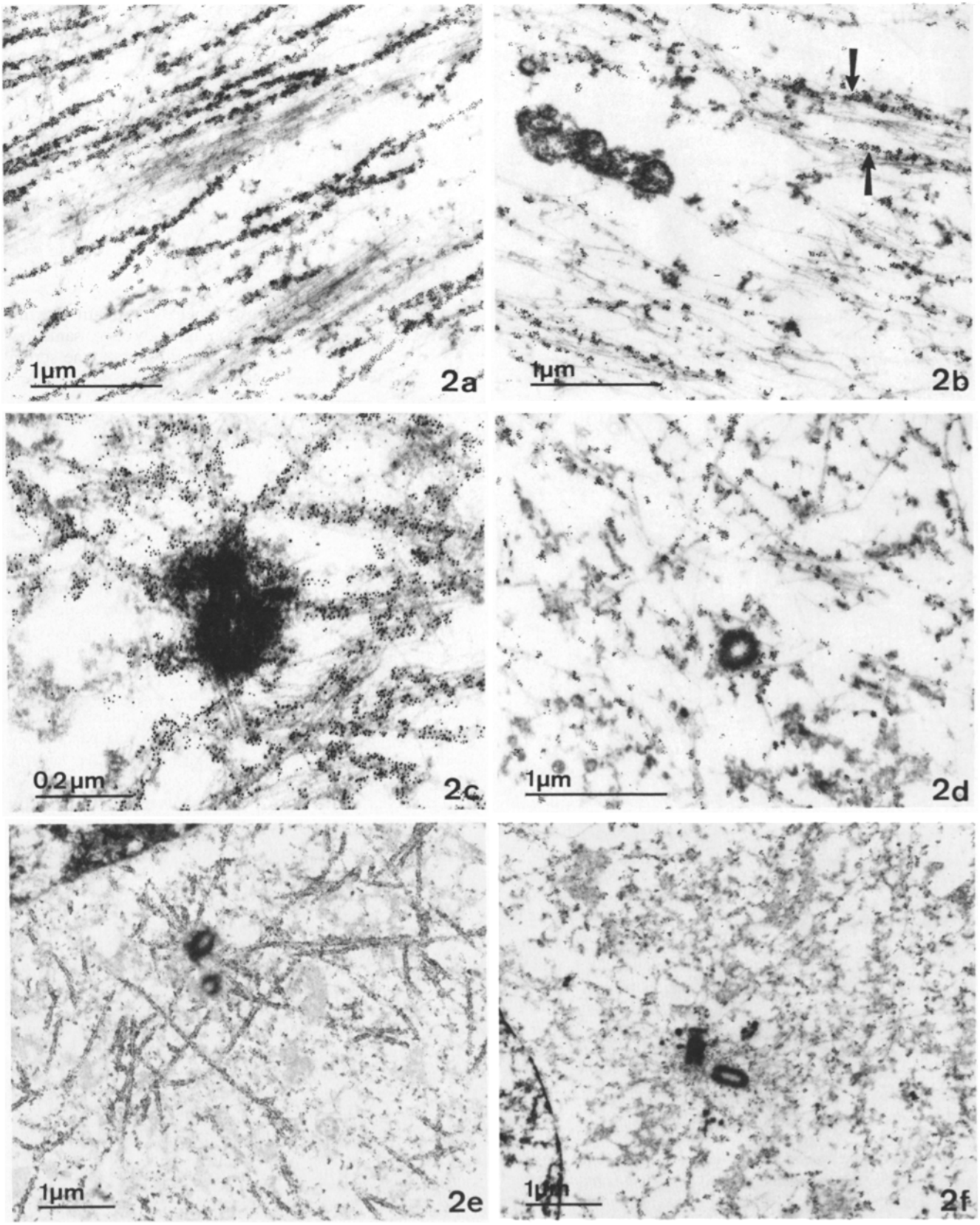

Figure 2. Electron microscopic immunogold staining of interphase cells. Staining was with Tyr (*left*) or Glu (*right*) rabbit antiserum followed by GAR-G5. (*a*) Peripheral region of CV_1 cell stained with Tyr antiserum. (*b*) Peripheral region of CV_1 cell stained with Glu antiserum. (*c*) Centrosomal area of CV_1 area stained with Tyr antiserum. (*d*) Centrosomal area of CV_1 area stained with Glu antiserum. (*e*) Centrosomal area of PtK_2 cell stained with Tyr antiserum. (*f*) Centrosomal area of PtK_2 cell stained with Glu antiserum. Arrows in *b* indicate nearly continuously Glu-stained microtubules.

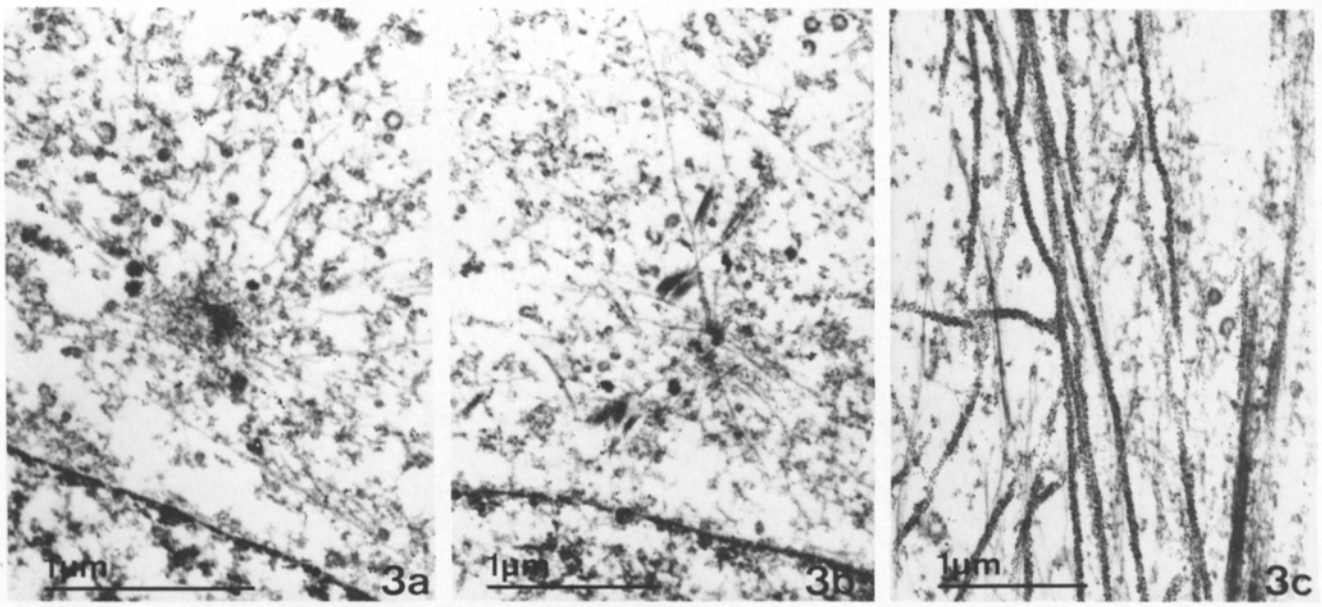

Figure 3. Controls for electron microscopic immunogold staining. PtK_2 interphase cells were stained with immune or preimmune serum (both at 1/200 dilutions) and then with GAR-G5. (*a*) Cell stained with Tyr preimmune serum. (*b*) Cell stained with Glu preimmune serum. (*c*) Cell treated with CPA (10 μg/ml for 30 min at 37°C [7]), before staining with Glu antiserum.

and Glu tubulin form complementary subsets of the tubulin in microtubules. The distribution of either size of gold particles along the microtubules seemed to be random; no evidence was found for ordered or periodic labeling with either antibody (see quantification below). Occasional patches of Glu reactivity were found along both interphase and mitotic microtubules (see arrowheads in Fig. 5, *a* and *d* [inset]); this had also been observed in Nanovid microscopy (Fig. 1).

Electron Microscopic Localization: Quantification

To determine if quantitative differences in the level of Tyr and Glu immunoreactivity could be detected in different classes of microtubules, we double-labeled cells as above and then determined the number of gold particles along microtubules (see Materials and Methods). In addition to any putative differences between interphase microtubules and different classes of spindle microtubules, we were interested in determining whether there was a difference between sinuous and straight interphase microtubules, since many of the microtubules brightly stained with the Glu antibody at the light microscopic level were sinuous (see Fig. 1, *d* and *f*; also reference 7). Fig. 6 shows examples from three of the classes of microtubules from PtK_2 cells in which we quantified the levels of Glu and Tyr immunoreactivity; it is clear that these three classes of microtubules show quantitatively different labeling, with the curly interphase microtubules (Fig. 6 *b*) having the highest levels of Glu immunoreactivity and the spindle microtubules (Fig. 6 *c*) having the lowest level of Glu immunoreactivity. Table I summarizes the results of these experiments and shows that there was a marked difference between the measured amount of Glu immunoreactivity in straight and in sinuous interphase microtubules. All classes of spindle microtubules possessed nearly the same levels of Glu immunoreactivity; notably, these levels were lower than those found in even the straight interphase microtubules.

Inspection of microtubules double-labeled with the Tyr and Glu antibodies suggested that the level of immunoreactivity with each antibody was relatively uniform along the length of a given microtubule. To examine this in more detail, we quantified the relative levels of Tyr and Glu immunoreactivity in short segments along individual microtubules that could be traced for >8 μm in a single thin section. Each microtubule was arbitrarily divided into segments of 0.7–1.0 μm and the number of each size of gold particle was determined. We analyzed seven microtubules (five Tyr-rich and two relatively Glu-rich) in this fashion; for both Tyr- and Glu-rich microtubules, we found that the relative level of Tyr and Glu immunoreactivity did not vary substantially from segment to segment of a single microtubule (Fig. 7). An occasional segment exhibited unusual reactivity when compared with other segments of the same microtubule (Fig. 7 *B*). This probably corresponds to the patchy labeling we occasionally observed, particularly with the Glu antibody (see Figs. 1 *f* and 5 *d*). We did not observe any consistent difference in the relative Tyr and Glu levels between segments near the centrosome and those near the cell periphery.

Discussion

We undertook the electron microscopic immunolocalization of Glu and Tyr tubulin to verify at high resolution and with better structural preservation the results obtained in previous light microscopic studies (7–9). These objectives have clearly been met; individual microtubules are resolved, and the relative levels of Tyr and Glu immunoreactivity along individual microtubules have been measured. In most respects, results described in this paper are similar to those we obtained by immunofluorescence: each form of α-tubulin was found to be heterogeneous in its distribution in cellular microtubules. Most microtubules showed weak reactivity with the Glu antibody and strong reactivity with the Tyr anti-

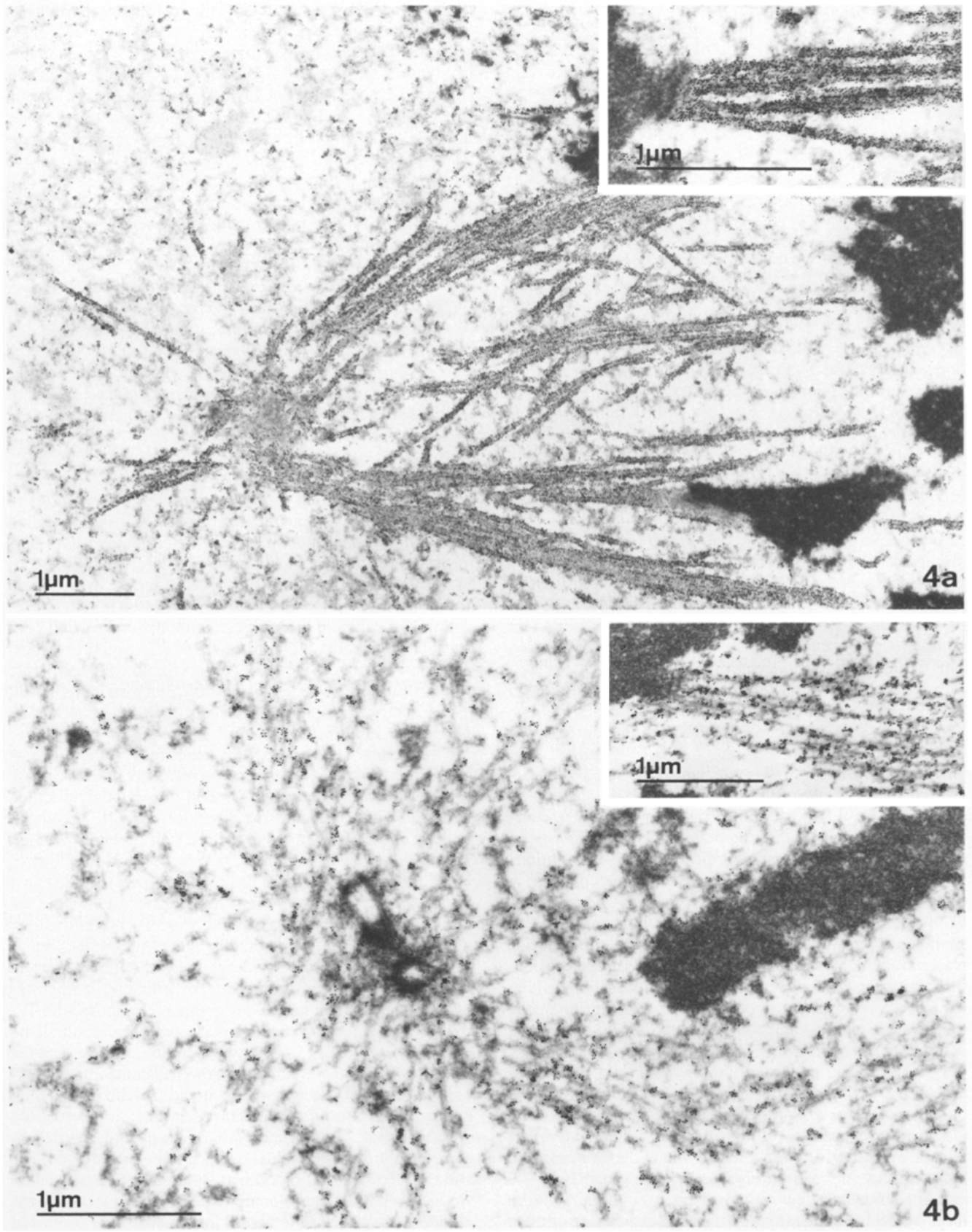

Figure 4. Electron microscopic immunogold staining of mitotic PtK_2 cells. Staining was with Tyr or Glu antisera and GAR-G5. (*a*) Half-spindle region stained with Tyr antibody. (*b*) Half-spindle region stained with Glu antibody. Insets in each panel show labeling of kinetochore microtubules. Kinetochores are the trilaminar structures at left.

Table I. Quantification of Tyr and Glu Immunoreactivity in PtK_2 Microtubules

Microtubule type	% Tyr	% Glu	Length*
			μm
Straight interphase	77 (71–91)	23 (9–29)	28.3
Wavy interphase	30 (17–47)	70 (53–83)	18.0
Straight centrosomal	79 (62–89)	21 (11–38)	11.1
Half-spindle	89 (80–96)	11 (4–20)	7.1
Aster	84 (73–89)	16 (11–27)	12.9
Kinetochore	84 (75–95)	16 (5–25)	7.5

Cells were double-labeled with Tyr and Glu antibodies, using 5-nm and 10-nm gold particles to detect Tyr and Glu immunoreactivity, respectively. Quantification was with a Quantimet image analyzer as described in Materials and Methods. The numbers in parentheses indicate the range (in %) of the individual determinations.

* Length is total length of microtubule segments used for quantification.

body, whereas for a minor population of sinuous microtubules the converse situation obtained. The latter type of microtubule was more prevalent in CV_1 than PtK_2 cells as determined at both the light and electron microscopic levels. Our electron microscopy also echoed our previous immunofluorescence (7) in that the amount of labeling with each antibody did not vary significantly over the length of a microtubule. A few localized patches of colloidal gold corresponding to Glu or Tyr reactivity were observed along microtubules (see discussion below); yet, if long segments of microtubules are considered, the overall levels are remarkably uniform (see Fig. 7). Thus, individual microtubules can be classified as "Glu-rich" or "Tyr-rich" by determining the number of gold particles in short segments of microtubules. The similarity in results obtained at both the light and electron microscopic levels legitimizes the use of the simpler technique of immunofluorescence for the qualitative assessment of Glu and Tyr tubulin distributions in cultured cells.

In the present study, every microtubule we examined at the electron microscopic level contained significant amounts of labeling with both the Tyr and Glu antibodies. This result differs significantly from our previous immunofluorescence results, in which some microtubules in double-labeled preparations were only stained with one of the two antibodies (7–9). This difference is probably due to the increased sensitivity and resolution of electron microscopic localization. (The difference is not due to the use of immunogold staining itself since the results obtained by immunofluorescence and Nanovid microscopy were similar.) Based on our previous immunofluorescence results, we concluded that cellular microtubules comprise a continuum of different compositions of Tyr and Glu tubulin and suggested that microtubules at the extremes might possess only one of the two species (7). The present results indicate that microtubules at the extremes are not composed of a single species, but are only substantially enriched for one of the species (see Table I). Nonetheless, the current results strengthen the idea that the levels of the two species vary widely in individual cellular microtubules. In fact, the broad range in the determination of Glu and Tyr percentages in individual interphase microtubules (see Table I) strongly supports the hypothesis that a broad continuum of Tyr and Glu levels exist in cellular microtubules.

Although we have quantified the Tyr and Glu levels in a limited population of microtubules, we consistently observed more Tyr immunoreactivity in straight microtubules than in morphologically sinuous microtubules in interphase cells. In fact, the relative percentage of Tyr immunoreactivity never exceeded 50% in sinuous microtubules, whereas the relative percentage of Glu never exceeded 40% in straight microtubules (see Table I). Sinuous microtubules had on the average about three times the relative amount of Glu immunoreactivity as did straight microtubules. These results are consistent with previous immunofluorescence studies (7, 9) and suggest that the generation of sinuous microtubules and Glu tubulin are tightly coupled processes.

The patchiness of the labeling with the Tyr, and especially, the Glu antibodies in the present study was not detected in previous immunofluorescence studies (7–9). We do not yet understand the significance of the patchy labeling; however, we favor the simple explanation that it reflects a regional heterogeneity in the distribution of the species within the microtubule. Such heterogeneity would occur if the enzyme that creates Glu tubulin, tubulin carboxypeptidase, acted locally at sites randomly distributed on the microtubule. It is also possible that the patchy labeling is an artifact of the antibody labeling itself. One result that argues against the latter explanation is the appearance of patches in double-labeled preparations in which the incubation with the two sizes of colloidal gold was done simultaneously. If patchy staining were caused by a random aggregation of gold particles during staining, these preparations should show "mixed" patches with two sizes of colloidal gold in each patch. In fact, such mixed patches were only rarely observed (see Fig. 5). In addition, the colloidal gold second antibodies we used did not contain sufficiently large aggregates (<5% triplets or larger) to account for all of the patches observed. To completely rule out labeling artifacts as the cause of patchy staining, it will be necessary to examine copolymers of Tyr and Glu tubulin assembled and labeled in vitro.

The method we have used to quantify Tyr and Glu immunoreactivity is extremely powerful, since it gives information about the levels of Tyr and Glu tubulin in single microtubules, while allowing this information to be related to other structural features of the cell (e.g., relative position of the microtubule, class of the microtubule, or proximity to other organelles). This is illustrated in perhaps the most striking result from the current study; each microtubule appears to have a single level of Glu (and Tyr) tubulin along its length (see Fig. 7). This finding places substantial limitations on any model for how microtubules of different Glu and Tyr compositions are generated. For example, if microtubules containing Glu tubulin are created from those with Tyr tubulin (see below), it requires that a whole microtubule be converted in concert. Similarly, it requires that the rate for such a Tyr to Glu conversion be slower than the rate of polymerization; otherwise, a gradient in the Tyr/Glu levels along a microtubule would have been observed.

Nonetheless, it is worth examining the quantitative data in some detail, before considering such hypotheses. It is clear that the relative levels of Tyr and Glu immunoreactivity that we have reported bear a complex relationship to the actual amounts of Tyr and Glu tubulin in a microtubule. Rothwell et al. found with brain–erythrocyte tubulin mixtures that the number of gold particles representing immunoreactivity with erythrocyte β-tubulin antibody was linear only up to ~25 mole percent erythrocyte β-tubulin; above this level

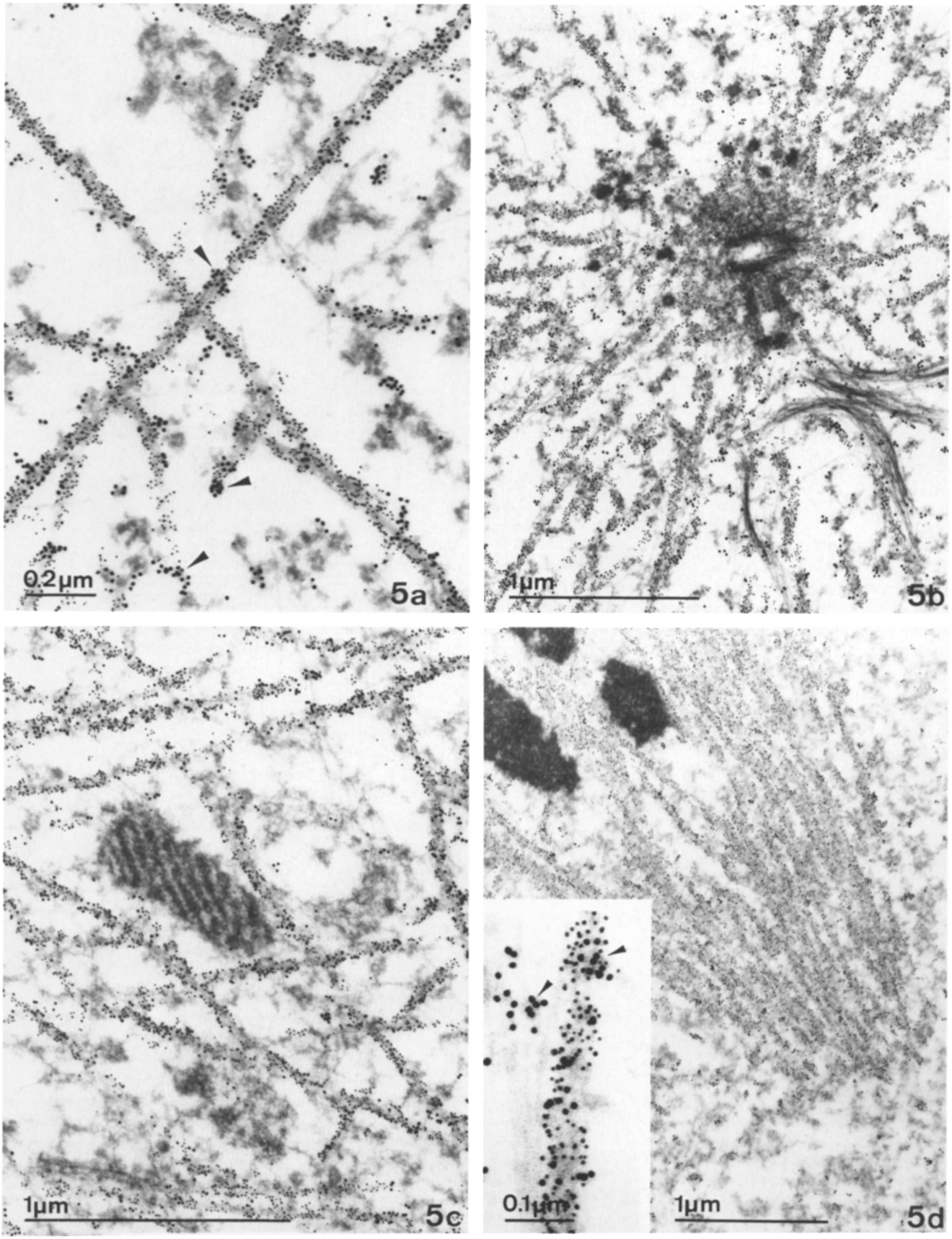

Figure 5. Electron microscopic immunogold staining: double-labeled cells. Cells were stained with Tyr antibody (rat monoclonal, YL 1/2, at a 1/200 dilution) and Glu rabbit antiserum (at a 1/200 dilution). Primary antibody reactivity was detected with GARa-G5 (5-nm particles for Tyr) and GAR-G10 (10-nm particles for Glu). (*a*) Interphase PtK_2 cell. Arrowheads indicate clusters of Glu immunoreactivity. (*b*) Spindle pole of a PtK_2 mitotic cell. (*c*) Interphase CV_1 cell. (*d*) Mitotic CV_1 cell showing half-spindle region. (*Inset*) Higher magnification of a spindle microtubule. Arrowheads indicate clusters of Glu immunoreactivity.

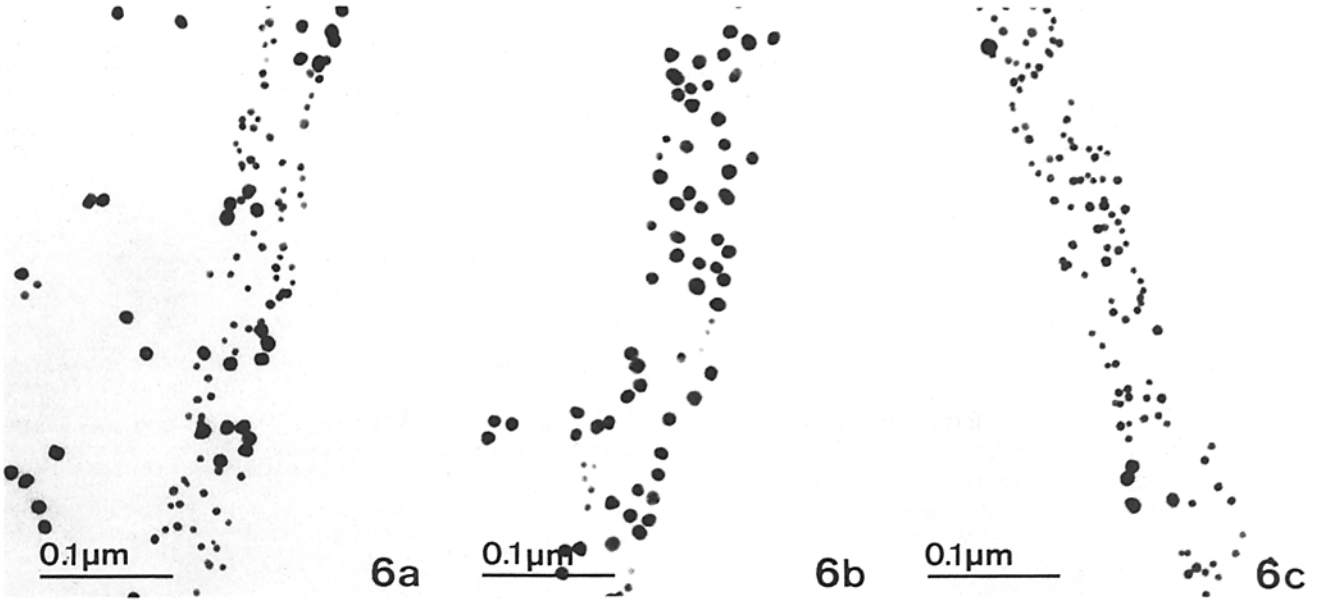

Figure 6. High magnification electron micrographs of double-labeled microtubules used for quantification. PtK_2 cells were double-labeled (as in Fig. 5) using 5-nm particles (GARa-G5) for Tyr staining and 10-nm particles (GAR-G10) for Glu staining. (*a*) Straight interphase microtubule. (*b*) Sinuous interphase microtubule. (*c*) Spindle microtubule.

saturation was observed (18). If an analogous situation exists for the Tyr and Glu antibodies, the relative percentage we have reported for microtubules with high levels of one of the species would be an underestimate of the actual percentage of the major species (and correspondingly, an overestimate of the actual percentage of the minor species). Furthermore, this suggests that for microtubules with approximately equal levels of Tyr and Glu immunoreactivity, a small change in the relative percentage may correspond to a substantial difference in the actual levels. For the relatively Glu-rich microtubule in Fig. 7 *B*, the levels of Tyr immunoreactivity in individual segments vary from 48 to 63% (ignoring for the moment the two segments with radically different relative Tyr/Glu levels). Although some of this variability is undoubtedly due to sampling errors associated with counting a small number of gold particles per segment, the actual differences in Tyr (or Glu) levels between segments is probably >15%. For the Tyr-rich microtubule in Fig. 7 *A*, the relative values are probably closer to the actual levels. Thus, only for microtubules that are enriched in one of the species can we be reasonably sure that the levels of Tyr (or Glu) tubulin are uniform along the length of a microtubule. For other microtubules, i.e., those with similar levels of Tyr and Glu tubulin, it will be necessary to extend this analysis to assess how much of the measured variability is due to actual variability in the Tyr and Glu levels and how much is due to variability in the determinations.

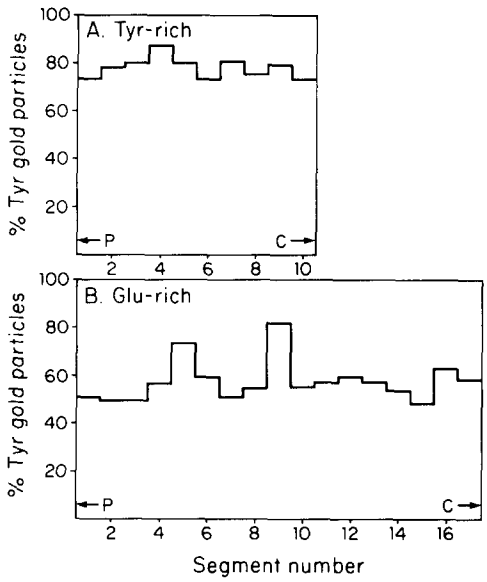

Figure 7. Quantification of relative levels of Tyr and Glu immunoreactivity along individual microtubules. Cells were double-labeled with Tyr and Glu antibodies (as in Fig. 5) and levels of immunoreactivity in arbitrarily divided segments along single microtubules were determined with a Quantimet image analyzer as described in the Materials and Methods. In *A*, (Tyr-rich microtubule) segments were 845 ± 44 nm; in *B*, (Glu-rich microtubule) segments were 877 ± 100 nm. Total length of the microtubule analyzed in *A* was 8,450 nm; that in *B* was 14,916 nm. *P* and *C* refer to the orientation of the microtubules with respect to the cell periphery and centrosome, respectively.

Results from the present study also add to our knowledge of Glu and Tyr tubulin distribution in the metaphase mitotic spindle. In light microscopic experiments, we had previously failed to detect Glu tubulin along astral microtubules at any stage and in the forming interzone during anaphase (8). Results from the present study clearly show that Glu tubulin is found in astral microtubules, albeit at a low level; we have also observed Glu tubulin in interzonal microtubules (unpublished observations). In fact, all classes of metaphase spindle microtubules showed approximately the same level of Glu and Tyr immunoreactivity, and somewhat surprisingly, the level of Glu immunoreactivity in these spindle microtubules was as low or lower than that present in all interphase microtubules of the same cell type (see Table I). This suggests that the bright immunofluorescent staining of the metaphase half-spindle observed previously with the Glu

antibody (7, 8) is due to tight packing of microtubules that possess low levels of Glu tubulin.

The significance of the relatively low level of Glu immunoreactivity and the nearly uniform distribution of each species in the metaphase spindle is presently unclear. We have recently obtained evidence that interphase Glu microtubules arise by post-polymerization modification of Tyr microtubules (manuscript in preparation). This implies that the level of Glu tubulin in a microtubule reflects the "age" (or time since nucleation) of that microtubule: the more Glu tubulin, the older the tubule. Thus, the relatively low level of Glu tubulin in the mitotic spindle is consistent with recent studies showing that spindle microtubules are turning over much more rapidly than interphase microtubules (10, 19, 20). Furthermore, the relatively uniform distribution of both Glu and Tyr tubulin in spindle microtubules of the stage we examined (metaphase) suggests that there are no substantial differences in the ages of these tubules. Since we have not examined all mitotic stages, the possibility still exists that microtubules in various classes of spindle fibers at stages of mitosis other than metaphase possess heterogeneous distributions of Glu tubulin, as our previous immunofluorescence study suggested (8).

The ability to quantify the relative amounts of Glu and Tyr immunoreactivity in individual microtubules by counting the number of the two sizes of gold particles will be extremely valuable in further studies on tyrosination/detyrosination. As described above, quantification has already shown that differences in levels of Glu and Tyr reactivity can be measured between classes of interphase tubules and between interphase and mitotic microtubules. Since we have obtained evidence that Glu microtubules are generated by post-polymerization modification of Tyr microtubules (manuscript in preparation), the ability to quantify time-dependent changes in the Glu and Tyr levels by this method will give us a means to measure the rate of interconversion of these two species under different conditions in vivo. The combination of specific antibody probes for species generated by posttranslational modification and detection using immunogold may be a useful approach for the quantification of in vivo rates of precursor–product reactions in other systems.

We thank Jan De Mey for his advice, Kathy Brill and Alan Strozer for careful and expedient typing of this manuscript, and Lambert Leyssen and Guy Jacobs for making the photographs. The rat monoclonal antibody against Tyr tubulin (YL 1/2) was a generous gift from Dr. J. V. Kilmartin.

This research was carried out during the tenure of a Postdoctoral Fellowship from the Muscular Dystrophy Association to G. G. Gundersen. This research was supported by grants from the National Institutes of Health (CA-39755) and the Muscular Dystrophy Association, a National Science Foundation Presidential Young Investigator Award to J. C. Bulinski and a grant from the IWONL (Brussels, Belgium) to M. DeBrabander.

Received for publication 19 March 1986, and in revised form 5 August 1986.

References

1. Arce, C. A., M. E. Hallak, J. A. Rodriguez, H. S. Barra, and R. Caputto. 1978. Capability of tubulin and microtubules to incorporate and to release tyrosine and phenylalanine and the effect of the incorporation of these amino acids on tubulin assembly. *J. Neurochem.* 31:205–210.

2. Barra, H. S., J. A. Rodriguez, C. A. Arce, and R. Caputto. 1973. A soluble preparation from rat brain that incorporates into its own proteins [^{14}C]-arginine by a ribonuclease-sensitive system and [^{14}C]-tyrosine by a ribonuclease-insensitive system. *J. Neurochem.* 20:97–108.

3. Barra, H. S., C. A. Arce, J. A. Rodriguez, and R. Caputto. 1974. Some common properties of the protein that incorporates tyrosine as a single unit into microtubule proteins. *Biochem. Biophys. Res. Commun.* 60:1384–1390.

4. Deanin, G. G., W. C. Thompson, and M. W. Gordon. 1977. Tyrosyl-tubulin ligase activity in brain, skeletal muscle, and liver of the developing chick. *Dev. Biol.* 57:230–233.

5. DeBrabander, M., J. C. Bulinski, G. Geuens, J. DeMey, and G. G. Borisy. 1981. Immunoelectron microscopic localization of the 210,000-mol-wt microtubule-associated protein in cultured cells of primates. *J. Cell Biol.* 91:438–445.

6. DeBrabander, M., R. Nuydens, G. Geuens, M. Moeremans, and J. De Mey. 1986. The use of submicroscopic gold particles combined with video contrast enhancement as a simple molecular probe for the living cell. *Cell Motil. Cytoskel.* 6:105–113.

7. Gundersen, G. G., M. H. Kalnoski, and J. C. Bulinski. 1984. Distinct populations of microtubules: tyrosinated and nontyrosinated alpha tubulin are distributed differently *in vivo*. *Cell.* 38:779–789.

8. Gundersen, G. G., and J. C. Bulinski. 1986. Distribution of tyrosinated and nontyrosinated alpha tubulin during mitosis. *J. Cell Biol.* 102:1118–1126.

9. Gundersen, G. G., and J. C. Bulinski. 1986. Microtubule arrays in differentiated cells contain elevated levels of a post-translationally modified form of tubulin. *Eur. J. Cell Biol.* In press.

10. Hamaguchi, Y., M. Toriyama, H. Sakai, and Y. Hiramoto. 1985. Distribution of fluorescently labeled tubulin injected into sand dollar eggs from fertilization through cleavage. *J. Cell Biol.* 100:1262–1272.

11. Kilmartin, J. V., B. Wright, and C. Milstein. 1982. Rat monoclonal antitubulin antibodies derived by using a new nonsecreting rat cell line. *J. Cell Biol.* 93:576–582.

12. Kumar, N., and M. Flavin. 1982. Modulation of some parameters of assembly of microtubules *in vitro* by tyrosinolation of tubulin. *Eur. J. Biochem.* 128:215–222.

13. Nath, J., and M. Flavin. 1979. Tubulin tyrosylation *in vivo* and changes accompanying differentiation of cultured neuroblastoma-glioma hybrid cells. *J. Biol. Chem.* 254:11505–11510.

14. Preston, S. F., G. G. Deanin, R. K. Hanson, and M. W. Gordon. 1981. Tubulin: tyrosine ligase in oocytes and embryos of *Xenopus laevis*. *Dev. Biol.* 81:36–42.

15. Raybin, D., and M. Flavin. 1977. Modification of tubulin by tyrosylation in cells and extracts and its effect on assembly *in vitro*. *J. Cell Biol.* 73:492–504.

16. Rodriguez, J. A., and G. G. Borisy. 1978. Modification of the C-terminus of brain tubulin during development. *Biochem. Biophys. Res. Commun.* 83:579–586.

17. Rodriguez, J. A., and G. G. Borisy. 1979. Tyrosination state of free tubulin subunits and tubulin disassembled from microtubules of rat brain tissue. *Biochem. Biophys. Res. Commun.* 89:893–899.

18. Rothwell, S. W., W. A. Grasser, and D. B. Murphy. 1986. End-to-end annealing of microtubules *in vitro*. *J. Cell Biol.* 102:619–627.

19. Salmon, E. D., R. J. Leslie, W. M. Saxton, M. L. Karow, and J. R. McIntosh. 1984. Spindle microtubule dynamics in sea urchin embryos: analysis using a fluorescein-labeled tubulin and measurements of fluorescence redistribution after laser photobleaching. *J. Cell Biol.* 99:2165–2174.

20. Saxton, W. M., D. L. Stemple, R. J. Leslie, E. D. Salmon, M. Zavortink, and J. R. McIntosh. 1984. Tubulin dynamics in cultured mammalian cells. *J. Cell Biol.* 99:2175–2186.

21. Wehland, J., M. C. Willingham, and I. V. Sandoval. 1983. A rat monoclonal antibody reacting specifically with the tyrosylated form of α-tubulin. I. Biochemical characterization, effects on microtubule polymerization *in vitro*, and microtubule polymerization and organization *in vivo*. *J. Cell Biol.* 97:1467–1475.